Tuning Probe-bilayer Architecture of Silver Nanoneedle-based Ion Channel Probes

Essraa A. Hussein,[§] Brittany Rice,[§] and Ryan J. White[§‡]*

[§] Department of Chemistry, University of Cincinnati, Cincinnati, OH 45221

[‡] Department of Electrical Engineering and Computer Science, University of Cincinnati, Cincinnati, OH 45221

ABSTRACT

Ion channel probes, as one of the ion channels platforms, provide an appealing opportunity to perform localized detection with high precision level. These probes come basically in two classes: glass and metal. While the glass-based probes showed the potential to be employed for molecular sensing and chemical imaging, these probes still suffer from limited resolution and lack of control over protein insertion. On the other hand, metal-based nanoneedle probes (gold and silver) have been recently developed to allow reducing probe dimensions to the nanoscale geometry. More specifically, silver probes are preferable owing to their ability to mitigate the channel current decay observed with gold probes and provide a DC stable channel current. However, there are still some challenges related to the probe design and bilayer curvature that render such probes insensitive to small changes in the tip-substrate distance. Herein, we introduce two main pathways to control the probe-bilayer architecture, the first is by altering the probe shape and geometry during the fabrication process of silver probes. The second pathway is by altering the surface characteristics of the silver probe via electrophoretic deposition process. Our findings reveal that varying the electrochemical etching parameters result in different probe geometries and producing sharper tips with two-fold diameter reduction. In addition, the electrophoretic deposition of a cathodic paint on the silver nanoneedle surface led to miniaturized exposed silver tip that enable the formation of a confined bilayer. We further investigated the characteristics of bilayers supported on both sharper nanoneedles and the HSR-coated silver probes produced from controlling the etching conditions and electrodeposition process,

respectively. We believe this work paves the way to rationally design silver nanoneedle ion channel probes, well-suited for localized molecular sensing and chemical imaging.

INTRODUCTION

Ion channel probes are an emerging nanopore platform which employs natural ion channels for molecular sensing and accurate localized detection at different interfaces.[1–5] These probes typically comprise a solid probe (glass or metal) that can support a lipid bilayer membrane at the tip sufficient for protein channel reconstitution and channel current measurements. The utilization of protein channel as a sensor element offers more opportunities to specifically detect small molecules or monitor the flux of specific ions with high spatial resolution.[1,6,7] Building off these advantages, ion channel probes have been applied to perform mapping of chemical flux across porous substrates with high specificity and signal-to-noise ratios.[2,3,5] While the ability of the glass-based ion channel probes has been demonstrated, there are still challenges related to the limited resolution of the micrometer-sized glass probe and the lack of control over protein insertion.[1,3,8]

An alternative support material for the fabrication of ion channel probes is a metal nanoneedle, which provides a potentially promising new means to perform molecular sensing with high spatial resolution. Metal nanoneedles (gold and silver) have been developed to address the current challenges of glass probes. The use of metal nanoneedles reduces the sensing tip diameter down to a nanoscale geometry (~200 nm), leading to enhanced spatial resolution for localized measurements.[8,9] We recently reported the advantage of silver nanoneedles over gold as the former exhibits a stable DC current resulting from the AgCl layer formed during the electrochemical etching of silver probes in a chloride-containing etchant.[9] Additionally, using such metal probes, especially silver, enabled control over the membrane area and the number of proteins inserted using the channel current as feedback to regulate the vertical displacement of the needle.[10] While we and others reported the feasibility of these metal probes to support ion

channel recordings,[9–14] there is still a need to rationally design the probe as well as the bilayer around the tip to extend its application as a imaging probe in scanning probe microscopy. In other words, the current metal probe architecture, with a cone-shaped tip, allows for a bilayer with curvature to be supported at the tip. This curved bilayer can lead to protein insertion away from the apex of the tip, and thus the ionic current obtained from these side proteins won't change when the probe approaches a substrate (see Figure 1). This means the current feedback obtained from such probes is insensitive to small changes in the tip-substrate distance (critical for the performance of scanning ion conductance measurements). Accordingly, there is a need to explore how different designs of metal probes and the subsequent formed bilayers can be controlled for specific use of the metal nanoneedle probes.

Herein, we introduce pathways to control the probe-bilayer architecture by altering the probe geometry and controlling where the lipid membrane can be formed around the silver tip (see Figure 1). First, we explored how different fabrication conditions of the silver nanoneedles during the etching process affect the resulting tip geometries and shape. Our findings reveal that a two-fold tip diameter reduction can be achieved via tuning electrochemical etching conditions. Then, we utilized an electrophoretic paint deposition process to miniaturize the exposed metal surface area of the silver probe and thus, form a confined bilayer around the miniaturized tip. Finally, we studied the characteristics of the bilayers supported on the different silver probes and the feasibility of different architectures to serve as an ion channel probe. This work paves the way to rationally design silver nanoneedle probes, suitable for diverse analytical applications.

EXPERIMENTAL

Chemicals and Reagents

For Silver nanoneedle fabrication, we used silver microwires of two diameters (250 μm and 100 μm) of 99.99% purity (Alfa Aesar), perchloric acid (70% $HClO_4$; Sigma-Aldrich), and

methanol (HPLC grade; Sigma-Aldrich). O-(3-carboxypropyl)-O′-[2-(3-mercaptopropionylamino) ethyl] propyl ethylene glycol (thiol PEG, MW 3000; Sigma-Aldrich) was used as ethanolic solution (ethanol proof, Decon Laboratories, Inc., PA, USA) for surface modification. An electrolyte/buffer solution was made of potassium chloride (KCl; Sigma-Aldrich) in a sodium phosphate buffer (pH 7.4) composed of sodium dihydrogen phosphate ($NaH_2PO_4 \cdot 2H_2O$; Sigma-Aldrich) and disodium phosphate (Na_2HPO_4, Sigma-Aldrich). The buffer solution was prepared using ultrapure water from a Milli-Q (Merck Millipore Corp.) resisted 18.2 MΩ at 25 °C. Electrophoretic paint (HSR cathodic paint; Clearclad Coatings, LLC, IL, USA) was used to insulate the silver nanoneedle- information about cathodic paints and HSR datasheet can be found at (Cathodic E-Coat - ClearClad Coatings, Inc.). For voltametric measurement, we used hexaammineruthenium(iii) chloride, 98% ($[Ru(NH_3)_6]^{2+}$, Sigma-Aldrich) and potassium nitrate (KNO_3, Sigma-Aldrich). Three different phospholipids were used to prepare the oil/lipid mixture and form the lipid bilayer; 1,2-Diphytanoyl-sn-glycero-3-phosphocholine (DPhPC), 1,2-dioleoyl-sn-glycero-3-phosphocholine (DOPC), and 1,2-dilinolenoyl-sn-glycero-3-phosphocholine (DLPC)- all lipids were purchased from Avanti Polar Lipids and mixed with n-decane (Merck Millipore Corp.). Alpha-hemolysin (αHL; Sigma-Aldrich) isolated from *Staphylococcus aureus* was used as a monomer protein powder.

Fabrication of silver nanoneedles of different geometries

Silver nanoneedle of average diameter 425 nm ± 33 nm was fabricated by electrochemical etching of a 250 μm silver wire using perchloric acid solution (perchloric acid : methanol, 1:4) as recently described in detail.[9] In order to tune the silver tip geometry and shape, we varied the etching conditions such as etching solution strength, etching voltage, and wire diameter. First, we used one step etching process using perchloric acid: methanol solutions with ratios; 1:2, 1:3, and 1:4 with applying a DC voltage of 1V to etch the 250 μm silver wire. For the 100 μm silver wire, we used etching solutions of perchloric acid: methanol in ratios; 1:4, 1:8, and 1:12 with applying a DC voltage of 1V. Second, we applied a two-step etching process, where a solution of perchloric

acid: methanol (1:3 and 1:4) were used in the first step and the second step, respectively. After etching, the silver tips were rinsed right after the etching with deionized water (80˚C) to eliminate the etching products and with acetone to clean up organic contaminants.[15] As we used 70% perchloric acid and mixed it with methanol in a ratio of 1:4, that means that the final concentration of perchloric acid is 14%. Similarly, when we change the ratio of perchloric acid to methanol to 1:12, 1:8, 1:3, and 1:2, the corresponding concentrations of the perchloric acid solutions are 5.4%, 7.8%, 17.5%, and 23.3%, respectively. To keep the expressions simple, we use the ratio formula in the figures as well as the results and discussions section. Methanol is used to reduce the bubbling effect during the etching process, leading to smooth surface close to the tip apex.[15,16]

Fabrication of insulated, electrophoretic painted silver nanoneedles

We used electrophoretic deposition technique to insulate the silver nanoneedle using a cathodic paint (HSR) according to the procedure mentioned in the literature.[17,18] The typical procedure we used here is by immersion of the etched silver nanoneedle (cathode) in HSR solution, and a DC voltage of 25 V was applied in the presence of carbon rod (anode) for 90 seconds. We also studied the effect of different voltages (ranges from 5 to 50V) and coating time (from 5s to 3 min) on the resulting coated tip. Then, the silver probe was rinsed with deionized water to remove any excess paint and left in the oven at 205˚C for 20 min to allow the paint to cure. After the heat curing, the HSR paint shrinks, leaving a small conductive apex exposed. The HSR-coated silver nanoneedles (HSR-coated AgNN) are then characterized to determine the tip radius.

Characterization of silver nanoneedles of different architectures

Scanning electron microscopy (Apreo SEM) operated at a voltage of 10 kV and an electron beam of 0.1 nA was employed to characterize the morphology of the fabricated silver nanoneedles with different geometries and the HSR-coated AgNN. We typically use the low-vac mode when

imaging the HSR-coated AgNN or otherwise, these probes are sputter coated with a thin layer of gold to render the whole surface conductive, suitable for the high-vac SEM. We also used electrochemical measurement (cyclic voltammetry and linear sweep voltammetry) to characterize the HSR-coated AgNN in a solution of 0.1M hexa-ammine ruthenium(iii) chloride in 1M KNO_3.

Formation of lipid bilayer and ion channel recordings

In this paper, we use two types of silver nanoneedles (AgNN); the first is named normal AgNN, referring to the etched silver nanoneedle in any etching conditions but without coating with electrophoretic paint. The second type is the HSR-coated AgNN, where that etched silver probe has been coated with the HSR cathodic paint using electrophoretic deposition method to insulate all the exposed silver surface except a small conductive apex at the tip. Both types were modified with Thiol PEG (MW 3000), which supports an aqueous electrolyte layer around the tip to be ready for measurements. We followed the detailed method we recently published to form the lipid bilayer.[8,9] Briefly, the silver probe is wetted in an electrolyte/buffer solution for few minutes and then inserted into a chamber with two compartments: oil/lipid phase (10 mg/mL of DPhPC, DOPC, or DLPC solution in n-decane) at the top and an aqueous buffered electrolyte bath solution of 1M KCl underneath the lipid compartment. Afterwards, the silver probe is mounted down to the chamber and then retracted up slowly to allow the formation of the first lipid monolayer around the tip at the oil/air interface. Then, with a second vertical movement of the tip down to the chamber, the monolayer around the tip combines with the monolayer at the oil/water interface to form the lipid bilayer at the lipid/aqueous interface and supported by the silver tip. After the formation of lipid bilayer, the αHL protein monomers in the electrolyte bath solution were reconstituted in the lipid membrane. Protein insertion was recognized by monitoring the ionic current, where each αHL channel results in a quantized current step of 100 pA when applying a potential of 100 mV in 1M KCl. All measurements were performed on an optical table and within a Faraday cage to reduce low frequency electronic ambient noise.

Membrane capacitance measurement

We measured the lipid membrane capacitance at different z positions and then, we find the membrane area using equation (1).[19–22]

$$C_{mem} = \frac{\varepsilon_{\circ}\, \varepsilon\, A}{d} \quad (1)$$

In equation (1), C_{mem} is the lipid membrane capacitance measured at different z positions using Pico2 Tecella amplifier, $\varepsilon_{\circ}$ is the permittivity of free space ($\varepsilon_{\circ}$ = 8.854 x10^{-14} F cm^{-1}), ε is the dielectric constant of the lipid bilayer (ε ~ 2.1), d is the thickness of bilayer, which is estimated to be 4nm [23–27] and A denotes to the surface area of the lipid membrane. We used equation (1) to calculate the surface area of different types of bilayers composed of lipids with different fluidities such as DPhPC, DOPC, and DLPC bilayers. Although the specific capacitance (C_M) can be used to characterize different lipids, it's the slope of a linear regression of the measured membrane capacitance versus membrane area- that means it's considered to be constant for every lipid when using the same oil composition at a constant temperature and zero dc voltage bias.[28–30] Accordingly, it's not the suitable parameter to use in the current study as we want to monitor the change of a parameter that changes with the change in the vertical movement of the silver probe, such as membrane capacitance (C_{mem}).

Instrumentation and data analyses

Ion channel recordings were collected using a Degan Chem-Clamp low-noise potentiostat (Minneapolis, MN) coupled to a PC using an in-house written LabVIEW program (National Instruments, Austin, TX). Controlling the probe displacement was achieved by a z-axis piezo actuator (PI (Physik Instruments) L.P., Auburn, MA) and a Multi-Micromanipulator Systems (MPC-200 controller and ROE). A patch-clamp amplifier (PICO 2, Tecella) with a 7.9 kHz low-pass filter at a sampling frequency of 40kHz was used to measure the membrane capacitance. In all

experiments, the silver nanoneedle probe acted as a working electrode (WE), while another Ag/AgCl wire inserted in the bath solution was used as a quasi-reference electrode (QRE). Data analyses including creating current time traces, current vs z-displacement plot, and bilayer area vs z-displacement were obtained using MATLAB R2019b and OriginPro 2017.

Results and Discussion

Silver nanoneedles exhibit great promise as ion channel probes that can be utilized for nanopore sensing, with a sustained, stable DC channel current. We recently reported the use of the silver-based ion channel probes to develop a current-regulated feedback mechanism to maintain long-term single channel recordings.[9,10] Although these probes enabled long-term stable channel current, there is still a challenge in the probe design that limits the extension of utilizing these probes for chemical imaging or scanning ion conductance microscopy (SICM). This challenge is related to the curved nature of the bilayer around the tip and subsequently, the protein location at the tip as shown in Figure 1. In order to address this challenge, a smaller or confined bilayer is needed to confine the protein location at the tip apex. In this study, we offer pathways to control the probe and bilayer architecture to be suitable for future applications. We investigated how different etching conditions would affect the fabricated silver probe geometry. In addition, we explored ways to control the bilayer formed around the tip and to form a confined bilayer around the silver nanoneedle tip.

Controlling silver nanoneedle tip shape and geometry

We use the electrochemical etching process to etch the silver microwires from the hundreds of micron range down to a few microns, submicron, or nanoscale ranges. The parameters regulating this electrochemical etching process are mainly the etching voltage, the etching solution strength, and the silver wire diameter.[15,31,32] Controlling the etched probe geometry and shape can be achieved by tuning these parameters. We previously reported the

use of 250 µm wire in a methanolic solution of perchloric acid (in a volume ratio of 1:4, perchloric acid: methanol, respectively) at a DC voltage of 1V to fabricate silver nanoneedle of 425 nm average diameter.[9] In this study, we vary the etching conditions applied for two different wire diameters; 100 µm and 250 µm wires to investigate how varying these conditions would affect the obtained probe geometry. For the 250 µm wires, we found that increasing the etching solution strength (perchloric acid: methanol) from 1:4 to 1:3 increased the tip diameter dramatically from 425 ± 33 nm to 5.6 ± 1.1 µm, as shown in Figure 2. We also investigated a two-step etching process, which means that the etching is performed first by immersing ~2mm of the silver microwire in a solution of perchloric acid: methanol (1: 3), then, immersing approximately half of the etched cone again into a solution of perchloric acid to methanol (1: 4) for a second etching step to produce tips with smaller geometries. The results of the two-step etching when applying a potential of 1V and 2V in the second step led to smaller tips with diameters of ~4 µm and 1 µm, respectively. It's noteworthy to mention that diluting the etching solution above the ratio of 1:4 (perchloric acid: methanol) resulted in longer etching time, and higher solution strength (less than 1: 3) cut off the wire without forming a cone-shaped tip. Additionally, when we explored the effect of varying the etching voltage from 1 V to 5 V, our findings revealed that higher voltage conditions lead to a faster reaction rate and short etching time but irregular or degraded tip quality (see Figure S1), in agreement with other reports for fabricating silver STM tips.[15,31] Accordingly, and for more consistency, we kept the etching voltage at 1 V and limited the use of 2 V to the second step in the two-step etching process.

For the 100 µm wire, we used more dilute etching solutions with ratios of 1: 8 and 1: 12, perchloric acid: methanol, respectively. Our findings demonstrated that the 1: 8 ratio resulted in a two-fold tip size reduction (diameter = 224 ± 38 nm), compared to our previously reported silver nanoneedle [9] as shown in Figure 2. On the other hand, using more dilute solutions such as 1: 12 produced a tip diameter of 460 ± 85 nm (see Figure 2). Although the two-step etching process

successfully produced reproducible tip geometries when starting with a 250 μm wire, this process, when applied to the 100 μm wire, did not yield consistent tip geometries. These findings show that tuning the electrochemical etching parameters, especially the voltage and the solution strength can result in the fabrication of silver probes with tip diameters ranging from 5 μm down to ~200 nm.

Ion channel current recordings and membrane capacitance measurements for bilayers formed on the 224 nm-diameter silver probes

One of the pathways we offer in this paper is the ability to control tip geometry and produce sharper tips that might allow for enhanced spatial resolution when employed as an ion channel probe. By varying etching conditions parameters, we were able to fabricate a silver tip of 224 nm diameter as shown in Figure 3. To investigate how the resulting sharper nanoneedle would serve as an ion channel probe, we first explored its ability to support ion channel recordings. Figure 3 shows the pore conductance of αHL channels (n = 24) in 1M KCl with applying a potential of 100 mV. The average value of pore conductance in these conditions was found to be 0.98 ± 0.21 nS, in agreement with values reported in the literature using the same conditions.[12,33,34] Second, we investigated the area of the lipid membranes supported on the sharper tips using phospholipids of different fluidities and compared it to the area obtained with lipid membranes supported on our previously reported silver nanoneedle of tip diameter ~425 nm[9] to investigate how the change in tip diameter would affect the resulting bilayer characteristics. We used three phospholipids of different fluidities: fully saturated phospholipid (DPhPC), unsaturated with two double bonds (DOPC), and unsaturated with six double bonds (DLPC). We measured the membrane capacitance (C_{mem}) of the bilayer formed from each phospholipid at different Z-positions by moving the silver probe up and down along a z-displacement of 300 μm. Then, we find the bilayer area corresponding to C_{mem} values at each z-position using equation (1). The schematic in Figure S2 demonstrates how the z-positioning is defined and how the change in C_{mem} is recorded during the

probe vertical movement. Figure 4 shows that the lipid bilayer area increases accordingly with moving the probe down across the oil/water interface but in a different way with each phospholipid. With the saturated and most stable lipid, we found no appreciable change in the membrane area between the sharper tip (224 nm tip diameter) and the original silver nanoneedle (425 nm diameter). However, when increasing the lipid fluidity, the lipid membrane supported on the sharper tips showed less area, compared to the original tips. We believe that this behavior of bilayer area change with pushing the silver probe into the oil/water interface is attributed to the way the bilayer is formed around the tip. The higher fluidity is attributed to the higher degree of unsaturation in the hydrocarbon chain of the fatty acid as the double bonds result in kinked lipid tails, occupying larger lateral surface area.[28,30,35] In addition, the higher fluid lipids are more disordered, less effectively packed, and more elastic, when compared to the more ordered, more tightly packed, and more rigid saturated lipid membranes.[36–38] Owing to the higher elasticity of the more fluid lipids, we refer the observed trend of bilayer area change in Figure 4 indicates that the bilayers of saturated lipids are more rigid and less conformed to the tip, while those of unsaturated lipids are fluid and more conformed to the tip shape. Accordingly, the most significant change in the membrane area was observed with the most fluid lipid used in this study (DLPC) as demonstrated in Figure 4. These results revealed that using sharper tips as ion channel probes can result in a smaller lipid membrane in the case of using fluid lipids but has no significant change on the area of the bilayer formed using DPhPC, the most stable and widely used lipid in ion channel recordings.[39]

Fabrication and Characterization of HSR-coated silver nanoneedles

Although our findings showed the ability to control the probe geometry and investigate how the bilayer changes with using sharper tips and fluid lipids, there's still a need to form a smaller or confined bilayer. Forming a confined bilayer at the probe tip can result in a bilayer with less curvature and confining the protein location at the tip apex, which will eventually pave the

way to extend the applications of silver nanoneedle probes. One of the ways we offer here to achieve this is by altering the surface chemistry of the silver metal probe by insulating part of the exposed metal. We employed an electrophoretic deposition technique, which has been previously utilized for miniaturizing electrodes to produce small electrode surfaces on the micro or nano scale.[17,18,40–42] The electrophoretic deposition process entails the application of an electric field that allows the charged particles of the electrophoretic paint to deposit onto one of the electrodes. We used a cathodic paint (HSR) to insulate the silver nanoneedle when applying a potential of 25 V for 90 s. The painted needles are then heat cured at 205˚C for 20 min to allow the shrinkage of the paint, leaving a small, exposed metal tip to be characterized.[18] Figure 5 shows the surface morphology of the HSR-coated silver nanoneedles in the SEM micrographs, distinguishing the light-colored small, exposed metal from the dark, insulated metal. Additionally, we performed electrochemical characterization of the HSR-coated silver nanoneedle by using voltammetry. The steady-state voltammetric response with a diffusion-limited current was observed with the reduction reaction of 1mM $Ru(NH_3)_6^{3+}$ in 1M KNO_3 as shown in Figure 5, compared to cyclic voltammogram for uncoated silver nanoneedle used as a control (see Figure S3). The steady-state or limiting current was measured at a scan rate of 50 mV/s, and the effective tip radius was estimated using equation (2), assuming the electrode geometry is hemispherical.[17,42]

$$I_{lim} = 2\,\pi\,n\,F\,D\,r\,C \qquad (2)$$

Where n is the number of electrons transferred per redox event, F is Faraday's constant, D and C are the diffusion coefficient and concentration of the electroactive species, respectively. Given $D = 8.6 \times 10^{-6}$ $cm^2\ s^{-1}$ for $Ru(NH_3)_6^{3+}$,[17,43] the voltammogram indicates an effective tip radius of ~ 19 μm as shown in Figure 5. The effective radius value estimated from steady-state voltametric response (~ 19 μm) was found to be higher than that measured from SEM micrograph (~11.5 μm). This is attributed to two factors associated with using the steady-state current response: an

assumed tip geometry (hemisphere despite the non-ideal shape of the ultrasmall electrode) and an assumed diffusion field although the flux of the species into the electrode surface can occur from all the electrode surroundings and extend beyond the ideal geometry of diffusion, leading to higher current and thus bigger estimated radius. However, using equation (2) of steady-state current is still useful to provide a rough estimation of the exposed surface area of the small electrodes.[42,44] The effective tip radii are calculated for other HSR-coated silver nanoneedles individually from SEM micrographs and steady state voltametric response as demonstrated in Figures S4 and S5 with different probes. Since the electrophoretic deposition process involves the movement of charged particles into an electrode, there are some parameters that control this process such as parameters related to the paint solution (e.g. concentration and electrophoretic mobility of the particles) and physical parameters (e.g. electric field strength, electrode surface area, and deposition time).[45–47] We studied different electrical parameters such as voltage and deposition time in order to ensure that the insulated part is well-covered without holes or defects and to allow for an exposed metal surface, enough to support bilayers and ion channel recordings. We found that the conditions for the ~1.5 cm exposed silver using the HSR cathodic paint are applying a voltage of 20 V to 25 V and deposition time of 60 to 90 s. Figure S6 shows that decreasing the applied potential (from 1 V to less than 20 V) or coating for short time (less than 60 s) resulted in imperfect coating with holes or cracking at the cone edge, especially with the silver probes prepared by the two-step etching process. Accordingly, we chose the conditions of 25 V and 90 s as the applied voltage and the coating time, respectively to produce the HSR-coated silver nanoneedle, suitable for ion channel recordings. Figure S7 shows SEM images for silver probes after performing the electrophoretic coating process with the as-mentioned conditions, compared to bare, non-coated silver probes prepared with the same electrochemical etching conditions. This figure demonstrates that there were no appreciable alterations to the original probe shape or geometry were observed after the electrophoretic coating.

Confined bilayers and channel current recordings using HSR-coated silver nanoneedles

To investigate how the new probe architecture of the HSR-coated silver nanoneedle would affect the feasibility of using it as an ion channel probe, we employed the HSR-coated silver nanoneedle probe to form a stable lipid membrane and to support the ion channel recordings. Figure 6 shows the quantized current steps of αHL protein pores when inserted into the lipid bilayer. This result shows the ability of the developed HSR-coated silver nanoneedle to support the ion channel despite the confined bilayer formed on the small, exposed silver tip. In order to characterize the confined bilayer supported on the HSR-coated silver tip, we measured the membrane capacitance to find the bilayer area using equation (1). Figure 7 shows the correlation between the change in the confined bilayer area with the Z-displacement of the probe, compared to the same measurement of the bilayer formed on uncoated normal silver nanoneedle. In the case of a bilayer formed on HSR-coated silver nanoneedle, we found that the membrane area reaches a plateau after a specific Z-distance and then, remained unchanged even with increasing the Z-displacement (i.e., keep moving the probe down). Contrarily, the values of membrane area for the uncoated, normal silver nanoneedle showed a continuous increase as the probe moves vertically down.[10] These findings demonstrate that the bilayer supported on the HSR-coated silver nanoneedle is confined on the miniaturized metal exposed after the electrophoretic deposition process, and has a much smaller area when compared to the normal silver nanoneedle probe. We believe that this introduces a rational design of silver nanoneedle probes, suitable not only for nanopore sensing but also for highly localized detection measurement and chemical imaging.

CONCLUSION

In this work, we introduce pathways to control probe and bilayer architecture of the silver nanoneedle-based ion channel probe. By varying the parameters of the electrochemical etching process, we can tune the probe geometry and obtain sharper tips with average diameter of 224 nm, that can be employed to support lipid bilayer and ion channel measurement. We studied the

characteristics of the supported bilayers formed of phospholipids of different fluidities. In addition, we altered the surface characteristics of silver nanoneedles by electrophoretic deposition of cathodic paint (HSR) to obtain miniaturized silver tip. The HSR-coated silver nanoneedle was characterized electrochemically, where it showed a steady-state voltammetric response. Finally, we demonstrated the feasibility of the HSR-coated silver tips with the small, exposed metal tip to form a confined bilayer, and thus can serve as ion channel probe that mitigates the problems associated with bigger bilayer curvatures when using normal silver nanoneedles. We believe this work offers more opportunities to rationally design metal-based ion channel probes, well-suited for diverse analytical applications.

ACKNOWLEDGMENTS

This material is based upon work supported by the National Science Foundation under Grant No. (CHE 2108368).

REFERENCES

(1) Zhou, Y.; Bright, L. K.; Shi, W.; Aspinwall, C. A.; Baker, L. A. Ion Channel Probes for Scanning Ion Conductance Microscopy. *Langmuir* **2014**, *30* (50), 15351–15355. https://doi.org/10.1021/la504097f.

(2) Shi, W.; Zeng, Y.; Zhou, L.; Xiao, Y.; Cummins, T. R.; Baker, L. A. Membrane Patches as Ion Channel Probes for Scanning Ion Conductance Microscopy. *Faraday Discuss.* **2016**, *193*, 81–97. https://doi.org/10.1039/c6fd00133e.

(3) Macazo, F. C.; White, R. J. Bioinspired Protein Channel-Based Scanning Ion Conductance Microscopy (Bio-SICM) for Simultaneous Conductance and Specific Molecular Imaging. *J. Am. Chem. Soc.* **2016**, *138*, 2793–2801. https://doi.org/10.1021/jacs.5b13252.

(4) Hussein, E. A.; Rice, B.; White, R. J. Recent Advances in Ion-Channel Probes for Nanopore Sensing: Insights into the Probe Architectures. *Anal. Chim. Acta* **2022**, *1224* (April), 1–11. https://doi.org/10.1016/j.aca.2022.340162.

(5) Shi, W.; Zeng, Y.; Zhu, C.; Xiao, Y.; Cummins, T. R.; Hou, J.; Baker, L. A. Characterization of Membrane Patch-Ion Channel Probes for Scanning Ion Conductance Microscopy. *Small* **2018**, *14*, 1–10. https://doi.org/10.1002/smll.201702945.

(6) Chen, C. C.; Zhou, Y.; Baker, L. A. Scanning Ion Conductance Microscopy. *Annu. Rev. Anal. Chem.* **2012**, *5*, 207–228. https://doi.org/10.1146/annurev-anchem-062011-143203.

(7) Zhu, C.; Huang, K.; Wang, Y.; Alanis, K.; Shi, W.; Baker, L. A. Imaging with Ion Channels. *Anal. Chem.* **2021**, *93* (13), 5355–5359. https://doi.org/10.1021/acs.analchem.1c00224.

(8) Shoji, K.; Kawano, R.; White, R. J. Spatially Resolved Chemical Detection with a Nanoneedle-Probe-Supported Biological Nanopore. *ACS Nano* **2019**, *13*, 2606–2614.

https://doi.org/10.1021/acsnano.8b09667.

(9) Hussein, E. A.; White, R. J. Silver Nanoneedle Probes Enable Sustained DC Current, Single-Channel Resistive Pulse Nanopore Sensing. *Anal. Chem.* **2021**, *93*, 11568–11575. https://doi.org/10.1021/acs.analchem.1c02087.

(10) Hussein, E. A.; White, R. J. Maintaining Single-Channel Recordings on a Silver Nanoneedle through Probe Design and Feedback Tip Positioning Control. *J. Phys. Chem. B* **2022**, *126* (48), 10111–10119. https://doi.org/10.1021/acs.jpcb.2c06275.

(11) Hirano, M.; Tomita, M.; Takahashi, C.; Kawashima, N.; Ide, T. Development of an Automated System to Measure Ion Channel Currents Using a Surface-Modified Gold Probe. *Sci. Rep.* **2021**, *11* (1), 1–9. https://doi.org/10.1038/s41598-021-97237-z.

(12) Shoji, K.; Kawano, R.; White, R. J. Analysis of Membrane Protein Deinsertion-Associated Currents with Nanoneedle-Supported Bilayers to Discover Pore Formation Mechanisms. *Langmuir* **2020**, *36* (34), 10012–10021. https://doi.org/10.1021/acs.langmuir.0c00833.

(13) Okuno, D.; Hirano, M.; Yokota, H.; Ichinose, J.; Kira, T.; Hijiya, T.; Uozumi, C.; Yamakami, M.; Ide, T. A Gold Nano-Electrode for Single Ion Channel Recordings. *Nanoscale* **2018**, *10*, 4036–4040. https://doi.org/10.1039/c7nr08098k.

(14) Okuno, D.; Hirano, M.; Yokota, H.; Onishi, Y.; Ichinose, J.; Ide, T. A Simple Method for Ion Channel Recordings Using Fine Gold Electrode. *Anal. Sci.* **2016**, *32*, 1353–1357. https://doi.org/10.2116/analsci.32.1353.

(15) Zhang, C.; Gao, B.; Chen, L. G.; Meng, Q. S.; Yang, H.; Zhang, R.; Tao, X.; Gao, H. Y.; Liao, Y.; Dong, Z. C. Fabrication of Silver Tips for Scanning Tunneling Microscope Induced Luminescence. *Rev. Sci. Instrum.* **2011**, *82* (8), 1–5. https://doi.org/10.1063/1.3617456.

(16) Iwami, M.; Uehara, Y.; Ushioda, S. Preparation of Silver Tips for Scanning Tunneling Microscopy Imaging. *Rev. Sci. Instrum.* **1998**, *69* (11), 4010–4011. https://doi.org/10.1063/1.1149215.

(17) Gray, N. J.; Unwin, P. R. Simple Procedure for the Fabrication of Silver/Silver Chloride Potentiometric Electrodes with Micrometre and Smaller Dimensions: Application to Scanning Electrochemical Microscopy. *Analyst* **2000**, *125* (5), 889–893. https://doi.org/10.1039/b001659o.

(18) Qiao, Y.; Chen, J.; Guo, X.; Cantrell, D.; Ruoff, R.; Troy, J. Fabrication of Nanoelectrodes for Neurophysiology: Cathodic Electrophoretic Paint Insulation and Focused Ion Beam Milling. *Nanotechnology* **2005**, *16* (9), 1598–1602. https://doi.org/10.1088/0957-4484/16/9/032.

(19) Alagappan, M.; Kandaswamy, A.; Kumaravel, M.; Rameshkumar, S. Interaction of Cholesterol with Artificial Bilayer Lipid Membrane System and Development of an Electrochemical Sensor. *Arab. J. Chem.* **2020**, *13*, 423–430. https://doi.org/10.1016/j.arabjc.2017.05.013.

(20) Steinem, C.; Janshoff, A.; Ulrich, W. P.; Sieber, M.; Galla, H. J. Impedance Analysis of Supported Lipid Bilayer Membranes: A Scrutiny of Different Preparation Techniques. *Biochim. Biophys. Acta - Biomembr.* **1996**, *1279*, 169–180. https://doi.org/10.1016/0005-2736(95)00274-X.

(21) Gentet, L. J.; Stuart, G. J.; Clements, J. D. Direct Measurement of Specific Membrane Capacitance in Neurons. *Biophys. J.* **2000**, *79*, 314–320. https://doi.org/10.1016/S0006-3495(00)76293-X.

(22) Heimburg, T. The Capacitance and Electromechanical Coupling of Lipid Membranes Close to Transitions: The Effect of Electrostriction. *Biophys. J.* **2012**, *103*, 918–929.

https://doi.org/10.1016/j.bpj.2012.07.010.

(23) Moellerfeld, J.; Prass, W.; Ringsdorf, H.; Hamazaki, H.; Sunamoto, J. Improved Stability of Black Lipid Membranes by Coating with Polysaccharide Derivatives Bearing Hydrophobic Anchor Groups. *BBA - Biomembr.* **1986**, *857*, 265–270. https://doi.org/10.1016/0005-2736(86)90355-X.

(24) Minamikawa, H.; Hato, M. Phase Behavior of Synthetic Phytanyl-Chained Glycolipid/Water Systems. *Langmuir* **1997**, *13*, 2564–2571. https://doi.org/10.1021/la961037t.

(25) Hirano-Iwata, A.; Niwano, M.; Sugawara, M. The Design of Molecular Sensing Interfaces with Lipid-Bilayer Assemblies. *TrAC - Trends Anal. Chem.* **2008**, *27*, 512–520. https://doi.org/10.1016/j.trac.2008.04.006.

(26) Enterohemorrhagic, F. A.; Erhardt, M.; Petra, C. The Impact of Plasma Membrane Lipid Composition on Flagellum-Mediated Adhesion of Enterohemorrhagic Escherichia Col. *msphere* **2020**, *5*, 702–720.

(27) Ermilova, I.; Swenson, J. DOPC: Versus DOPE as a Helper Lipid for Gene-Therapies: Molecular Dynamics Simulations with DLin-MC3-DMA. *Phys. Chem. Chem. Phys.* **2020**, *22*, 28256–28268. https://doi.org/10.1039/d0cp05111j.

(28) Taylor, G. J.; Venkatesan, G. A.; Collier, C. P.; Sarles, S. A. Direct in Situ Measurement of Specific Capacitance, Monolayer Tension, and Bilayer Tension in a Droplet Interface Bilayer. *Soft Matter* **2015**, *11* (38), 7592–7605. https://doi.org/10.1039/c5sm01005e.

(29) Velikonja, A.; Kramar, P.; Miklavčič, D.; Maček Lebar, A. Specific Electrical Capacitance and Voltage Breakdown as a Function of Temperature for Different Planar Lipid Bilayers. *Bioelectrochemistry* **2016**, *112*, 132–137.

https://doi.org/10.1016/j.bioelechem.2016.02.009.

(30) Venkatesan, G. A.; Taylor, G. J.; Basham, C. M.; Brady, N. G.; Collier, C. P.; Sarles, S. A. Evaporation-Induced Monolayer Compression Improves Droplet Interface Bilayer Formation Using Unsaturated Lipids. *Biomicrofluidics* **2018**, *12*, 024101–024113. https://doi.org/10.1063/1.5016523.

(31) Lloyd, J. S.; Williams, A.; Rickman, R. H.; McCowen, A.; Dunstan, P. R. Reproducible Electrochemical Etching of Silver Probes with a Radius of Curvature of 20 Nm for Tip-Enhanced Raman Applications. *Appl. Phys. Lett.* **2011**, *99* (14), 1–4. https://doi.org/10.1063/1.3646106.

(32) Hobara, R.; Yoshimoto, S.; Hasegawa, S.; Sakamoto, K. Dynamic Electrochemical-Etching Technique for Tungsten Tips Suitable for Multi-Tip Scanning Tunneling Microscopes. *e-Journal Surf. Sci. Nanotechnol.* **2007**, *5* (April), 94–98. https://doi.org/10.1380/ejssnt.2007.94.

(33) Bhattacharya, S.; Muzard, L.; Payet, L.; Mathe, J.; Bockelmann, U.; Aksimentiev, A.; Viasnoff, V. Rectification of the Current in Alpha-Hemolysin Pore Depends of the Cation Type: The Alkali Series Probed by MD Simulations and Experiments. *J Phys Chem* **2011**, *115*, 4255–4264. https://doi.org/10.1021/jp111441p.Rectification.

(34) Oukhaled, G.; Bacri, L.; Mathé, J.; Pelta, J.; Auvray, L. Effect of Screening on the Transport of Polyelectrolytes through Nanopores. *Europhys. Lett.* **2008**, *82*, 48003-p1-48003-p5. https://doi.org/10.1209/0295-5075/82/48003.

(35) Huang, Y.; Fuller, G. G.; Chandran Suja, V. Physicochemical Characteristics of Droplet Interface Bilayers. *Adv. Colloid Interface Sci.* **2022**, *304* (April), 1–15. https://doi.org/10.1016/j.cis.2022.102666.

(36) Smaby, J. M.; Kulkarni, V. S.; Momsen, M.; Brown, R. E. The Interfacial Elastic Packing Interactions of Galactosylceramides, Sphingomyelins, and Phosphatidylcholines. *Biophys. J.* **1996**, *70* (2 I), 868–877. https://doi.org/10.1016/S0006-3495(96)79629-7.

(37) Epand, R. M.; Epand, R. F. Lipid Domains in Bacterial Membranes and the Action of Antimicrobial Agents. *Biochim. Biophys. Acta - Biomembr.* **2009**, *1788* (1), 289–294. https://doi.org/10.1016/j.bbamem.2008.08.023.

(38) Nowotarska, S. W.; Nowotarski, K. J.; Friedman, M.; Situ, C. Effect of Structure on the Interactions between Five Natural Antimicrobial Compounds and Phospholipids of Bacterial Cell Membrane on Model Monolayers. *Molecules* **2014**, *19* (6), 7497–7515. https://doi.org/10.3390/molecules19067497.

(39) Kara, S.; Afonin, S.; Babii, O.; Tkachenko, A. N.; Komarov, I. V.; Ulrich, A. S. Diphytanoyl Lipids as Model Systems for Studying Membrane-Active Peptides. *Biochim. Biophys. Acta - Biomembr.* **2017**, *1859*, 1828–1837. https://doi.org/10.1016/j.bbamem.2017.06.003.

(40) Watkins, J. J.; Chen, J.; White, H. S.; Abruña, H. D.; Maisonhaute, E.; Amatore, C. Zeptomole Voltammetric Detection and Electron-Transfer Rate Measurements Using Platinum Electrodes of Nanometer Dimensions. *Anal. Chem.* **2003**, *75* (16), 3962–3971. https://doi.org/10.1021/ac0342931.

(41) Schulte, A.; Chow, R. H. A Simple for Insulating Microelectrodes Using Anodic Electrophoretic Deposition of Paint. *Anal. Chem.* **1996**, *68* (17), 3054–3058. https://doi.org/10.1021/ac960210n.

(42) Conyers, J. L.; White, H. S. Electrochemical Characterization of Electrodes with Submicrometer Dimensions. *Anal. Chem.* **2000**, *72* (18), 4441–4446. https://doi.org/10.1021/ac000399+.

(43) Liu, F.; Kolesov, G.; Parkinson, B. A. Time of Flight Electrochemistry: Diffusion Coefficient Measurements Using Interdigitated Array (IDA) Electrodes. *J. Electrochem. Soc.* **2014**, *161* (13), H3015–H3019. https://doi.org/10.1149/2.0041413jes.

(44) Bard, Allen J.; Faulkner, L. R. *Electrochemical Methods: Fundamentals and Applications*; John Wiley & Sons, 2001.

(45) Zhitomirsky, I.; Gal-Or, L. Electrophoretic Deposition of Hydroxyapatite. *J. Mater. Sci. Mater. Med.* **1997**, *8* (4), 213–219. https://doi.org/10.1023/a:1018587623231.

(46) Wang, Y. C.; Leu, I. C.; Hon, M. H. Kinetics of Electrophoretic Deposition for Nanocrystalline Zinc Oxide Coatings. *J. Am. Ceram. Soc.* **2004**, *87* (1), 84–88. https://doi.org/10.1111/j.1551-2916.2004.00084.x.

(47) Besra, L.; Liu, M. A Review on Fundamentals and Applications of Electrophoretic Deposition (EPD). *Prog. Mater. Sci.* **2007**, *52* (1), 1–61. https://doi.org/10.1016/j.pmatsci.2006.07.001.

FIGURES

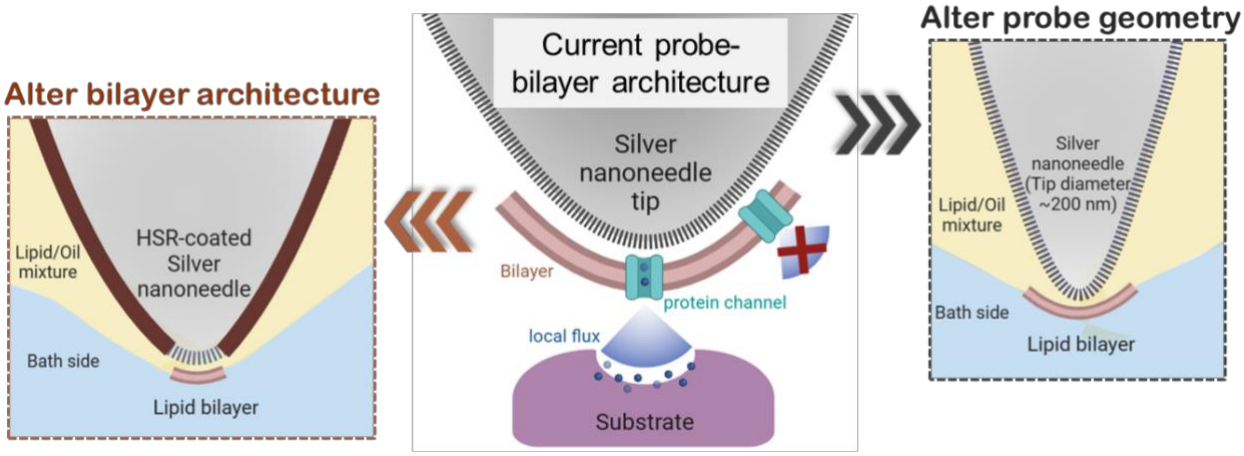

Figure 1. Schematic diagram illustrates ways to control the probe-bilayer architecture. (Middle) Our normal silver nanoneedle with a tip diameter 425 nm shows the effect of the curved bilayer on the protein location and thus, on the ability to employ such probes for localized detection measurement. (Right) Sharper silver tip with 224 nm diameter fabricated by controlling silver etching conditions. (Left) HSR-coated silver nanoneedle produced by electrophoretic deposition of cathodic paint (HSR) into the etched silver probe, developed to form a confined bilayer.

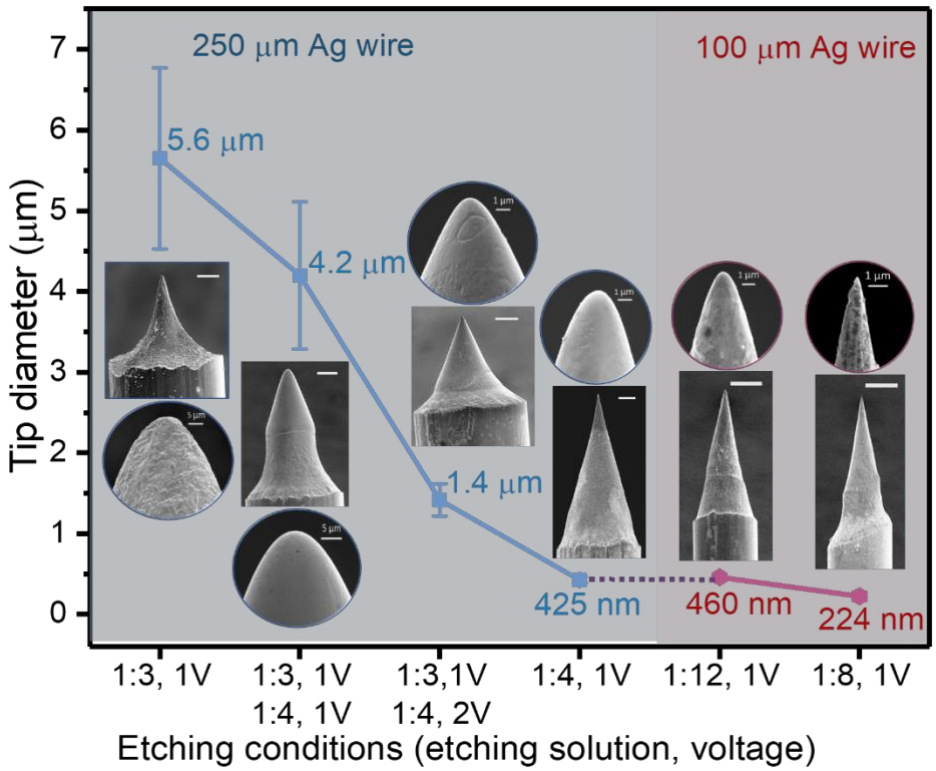

Figure 2. Tip diameter control via varying electrochemical etching conditions of silver microwires. The ratios shown on x-axis are for the etching solution strength (perchloric acid: methanol). Rectangle images are low magnification SEM micrographs corresponding to each etching condition with scale bar of 50 μm. Rounded images are the corresponding high magnification SEM micrographs. Tip diameter for each etching condition is an average of six silver probes prepared using the same etching parameters.

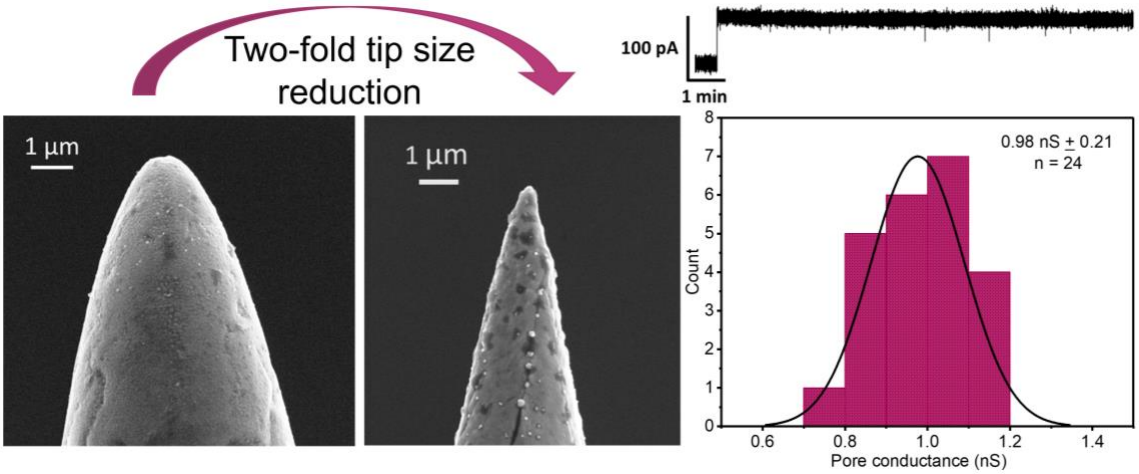

Figure 3. Surface morphology and ion channel recordings for the two-fold sharper tips (224 nm diameter). (Left) SEM micrographs for silver nanoneedle tip of both 425 nm diameter and the sharper 224 nm tip, respectively. (Right, top) Single open channel current for αHL protein pore in 1M KCl. (Right, bottom) Measured conductance for 24 αHL channels at a potential of 100mV when using sharper silver nanoneedles of 200 nm tip diameter as ion channel probe. The mean pore conductance value was 0.98 ± 0.21 nS.

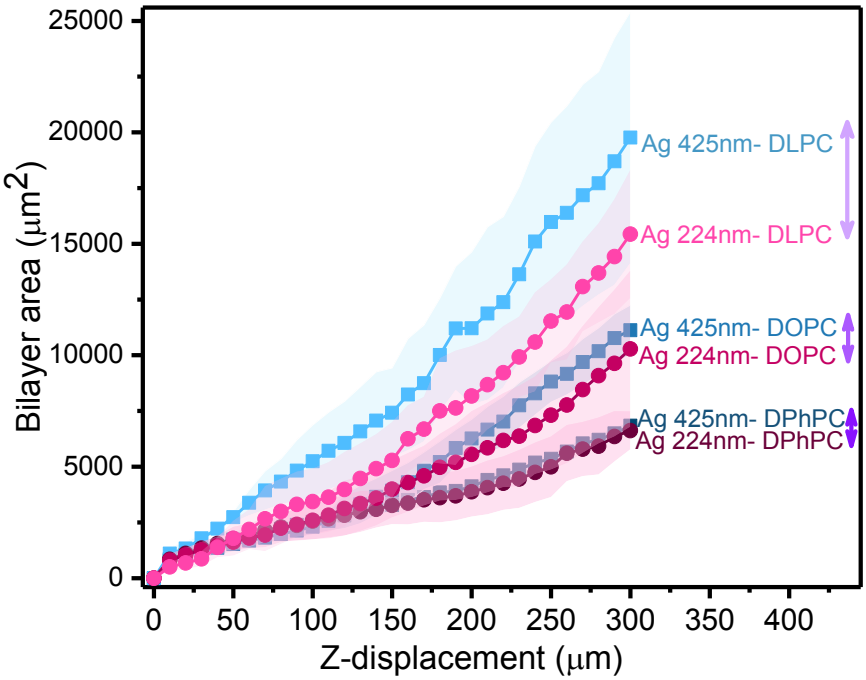

Figure 4. Lipid membrane area measurement vs Z-displacement for the sharper 224 nm silver nanoneedle tips obtained from this work (three pink traces) using three phospholipids of different fluidities, compared to our previously published results of membrane area obtained using the 425 nm silver nanoneedle tips (three blue traces).[10] The shaded areas in the graph represent the standard deviation for three silver probes with three replicate measurements for each Ag 425 nm probe and five silver probes with three replicates for each Ag 224 nm probe.

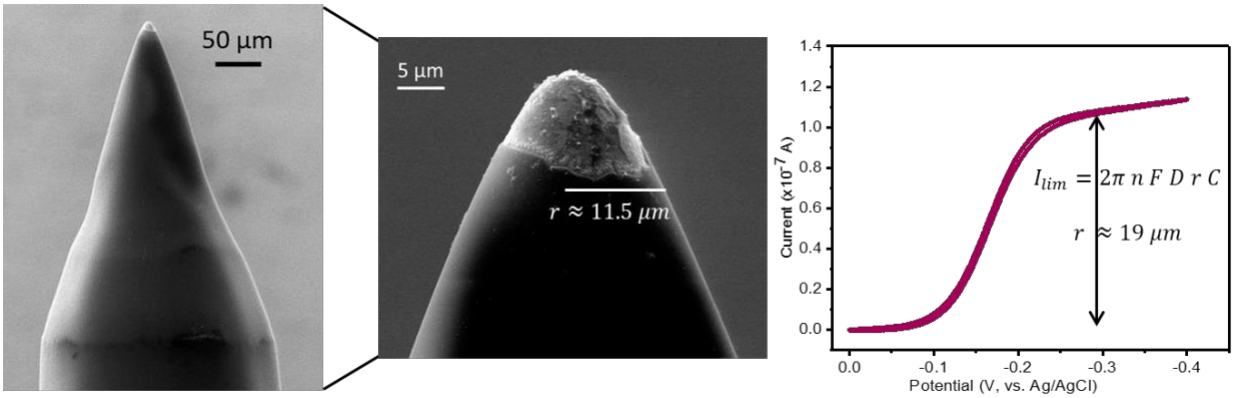

Figure 5. Characterization of HSR-coated silver nanoneedle, fabricated by electrophoretic coating of silver nanoneedle. (Left and middle) SEM micrograph for the HSR-coated silver nanoneedle shows the different morphology at low and high magnification. (Right) Cyclic voltammogram shows the steady state current response of the HSR-coated silver nanoneedle when it was used as a working electrode for one electron redox reaction of 1mM hexamine ruthenium (iii) chloride in 1M KNO_3.

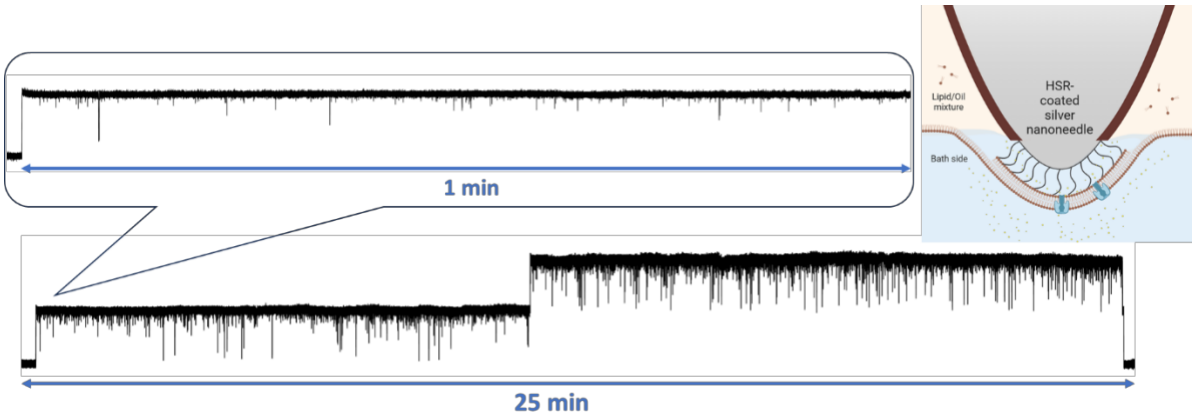

Figure 6. Ion channel recordings using HSR-coated silver nanoneedle demonstrate the feasibility of this probe to support DC stable open channel current for αHL proteins inserted in a confined bilayer.

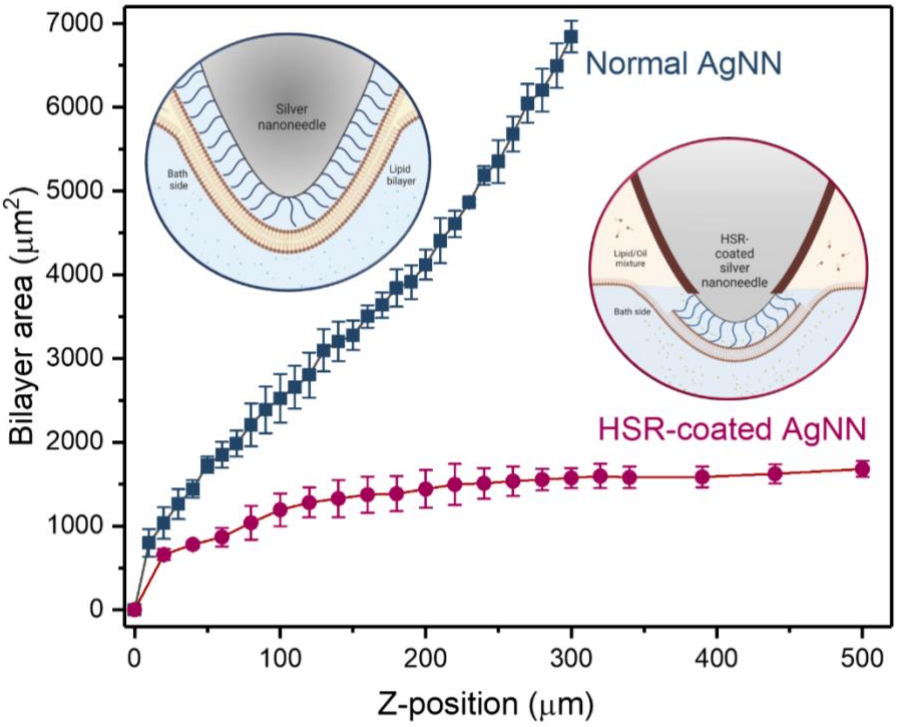

Figure 7. Lipid membrane area vs Z-displacement for the confined bilayer supported on the HSR-coated silver nanoneedle (dark red trace), compared to our previously published results of normal silver nanoneedle of 425 nm tip diameter using DPhPC lipid (dark blue trace)[10]. The bilayer area was measured for three silver tips with three readings for each normal AgNN and six probes with three replicate readings for each HSR-coated AgNN.

TOC

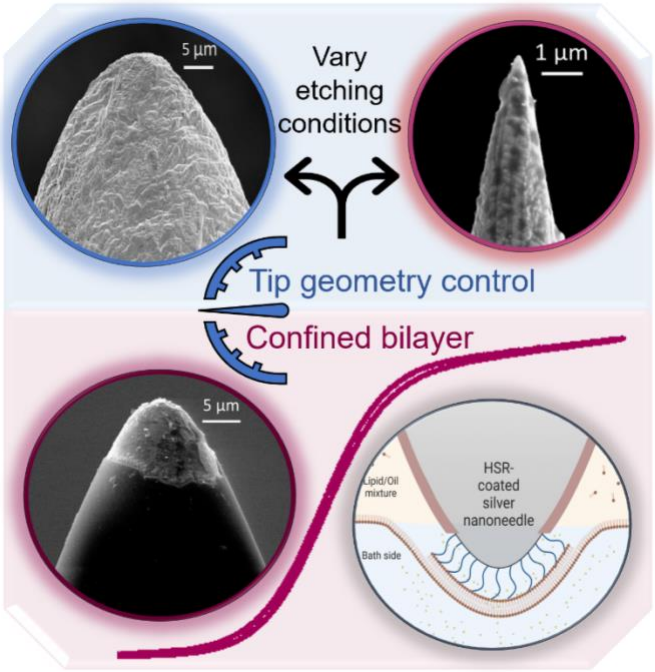
5 µm
Vary
etching
conditions
1 µm
Tip geometry control
Confined bilayer
5 µm
Lipid/Oil
mixture
HSR-
coated
silver
nanoneedle
Bath side